

Closed Loop Controlled Bidirectional DC-DC Converter with the Coupled Inductor

*K.C. Ramya *V. Jegathesan

Abstract : In the present work, reduction of ripple in the output of bidirectional DC-DC converter is presented. This Converter has the ability to transfer the energy in both the directions. The proposed converter has been modeled in order to carry out the simulation by means of MATLAB SIMULINK. The Pi-filter has been introduced at the output so as to reduce the peak to peak ripple as much as possible. The simulation is done with and without PI controller and the simulation results of the closed loop system have been furnished.

Keywords : Bidirectional DC-DC converter, Coupled Inductor, Matlab Simulink.

1. INTRODUCTION

Bidirectional DC-DC converters (BDC) are widely used in many applications such as renewable energy sources, hybrid electric vehicles, battery chargers etc., [1-9]. However the voltage gain is limited by various facts such as power switches, inductor and capacitor. The high step up and step down voltage gain can be obtained from isolated converter by tuning the ratio of the transformer [11]. It results in high voltage stress on switches which in turns lead to low efficiency. In non-isolated bidirectional DC-DC converters such as multilevel type require twelve switches. For the requirement of high step-up and step-down voltage gains, more number of switches has to be added. This makes the circuit more complicated. In three-level type, the voltage stress on the switches is only half of the conventional type [10]. But the step-up and step-down voltage gains are low. In SEPIC/zeta type, the conversion efficiency is low because it is a combination of two power stages. The switched capacitor and coupled inductor type can afford high step up and step down voltage gains but their circuit configuration is very complicated [12-20]. A conventional bidirectional converter with coupled inductor is shown in Fig. 1.

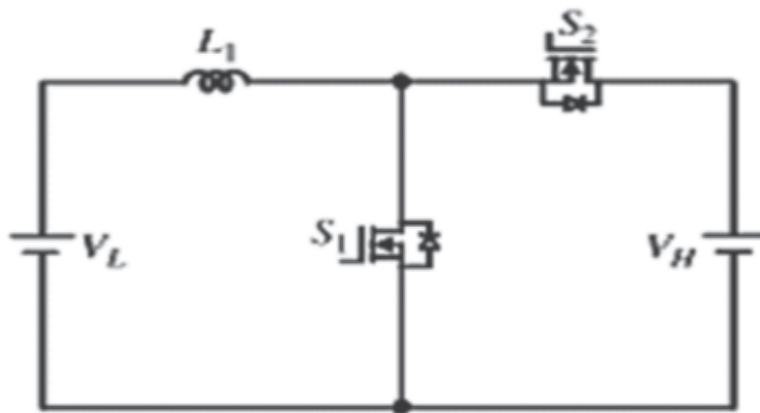


Fig. 1. Conventional BDC Boost/Buck Converter

This converter is very simple. But it has the problem of the voltage and current ripples at its input and output. Hence, a large capacitor or inductor filters are required to suppress the ripples. But this results in high loss and low efficiency. Hence in order to overcome this drawback of the conventional converter, a novel bidirectional converter [19-30] is proposed as shown in Fig.2.

* Department of Electrical and Electronics Engineering, Karunya University, Coimbatore, India, Corresponding Author: ramya2614@gmail.com

The Proposed converter consist of two switches namely S1 and S2, a coupled inductor with same winding turns in the primary and secondary. S3 is the synchronous rectifier. The proposed converter provides: 1) Higher step-up and step-down voltage gains and 2) lower average value of the switch current under same electric specifications. The on-state resistance $R_{DS(ON)}$ of the switches and the equivalent series resistances of the coupled inductor and capacitors are ignored; the capacitor is sufficiently large; and the voltages across the capacitor can be treated as constant.

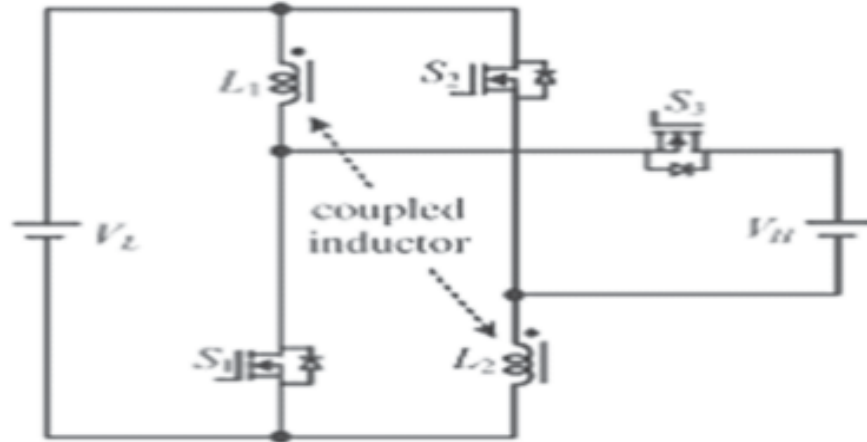


Fig. 2. Proposed Bidirectional DC-DC Converter

Existing filter is replaced by a Pi-filter to reduce the ripple. The above literature does not deal with the modeling of the closed loop controlled bidirectional DC-DC converter. This work proposes a model for closed loop controlled DC-DC converter system. This paper is organized as follows: Section 2 deals with the modes of operation of bidirectional DC-DC converter. Discussion on simulation results is presented in the third section. The work is concluded in the fourth section.

2. STEP-UP MODE

The proposed converter in step-up mode is shown in Fig.3. The switches S1 and S2 are controlled by pulse width modulation (PWM) technique simultaneously.

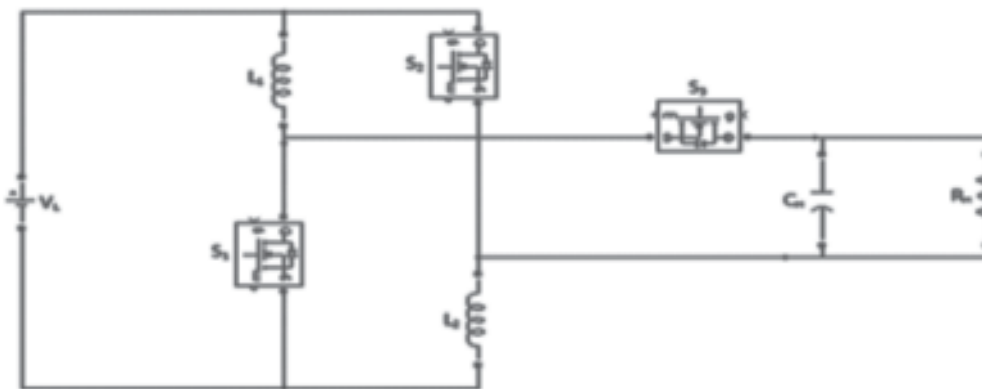


Fig. 3. Proposed converter in step-up mode

Thus, the inductance of the coupled inductor can be expressed as

$$L_1 = L_2 = L \tag{1}$$

$$M = K\sqrt{(L_1L_2)} = KL \tag{2}$$

The mutual inductance M of the coupled inductor is given by

Where k is the coupling co-efficient of coupled inductor. Hence the voltage across the primary and secondary winding of the coupled inductor can be expressed as

$$V_{L_1} = L_1 \frac{di_{L_1}}{dt} + M \frac{di_{L_2}}{dt} = L \frac{di_{L_1}}{dt} + kL \frac{di_{L_2}}{dt} \tag{3}$$

$$V_{L_2} = L_1 \frac{di_{L_1}}{dt} + L_2 \frac{di_{L_2}}{dt} = kL \frac{di_{L_1}}{dt} + kL \frac{di_{L_2}}{dt} \tag{4}$$

Mode I : During this mode, Switch S_1 and S_2 are ON and S_3 is in OFF condition, as shown in fig.3(a).

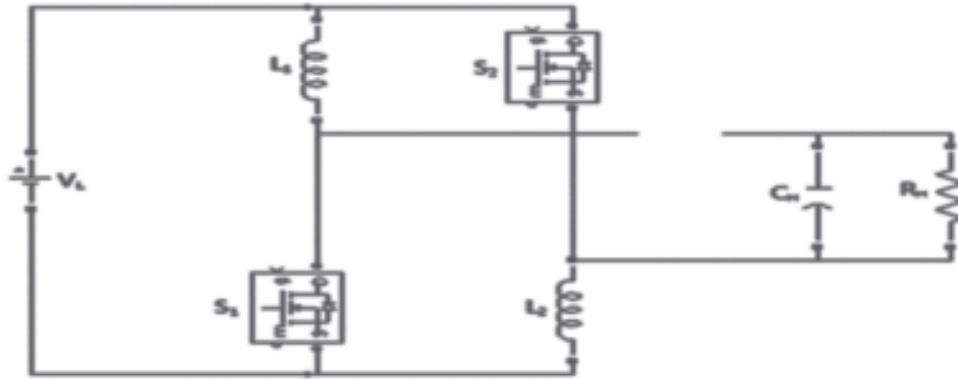


Fig. 3(a). Proposed Converter in Mode 1.

Hence, the low voltage side V_L is transferred to the coupled inductor and the energy stored in the capacitor C_H is discharged to the load. Thus the voltage across L_1 and L_2 are obtained as follows

$$v_{L_1} = v_{L_2} = v_L \tag{5}$$

Substituting (3) and (4) into (5), yielding

$$\frac{di_{L_1}(t)}{dt} = \frac{di_{L_2}(t)}{dt} = \frac{V_L}{(1+k)}, t_0 \leq t \leq t_1 \tag{6}$$

Mode II : During this mode, switches S_1 and S_2 are OFF and S_3 is ON condition as shown in Fig.3(b).

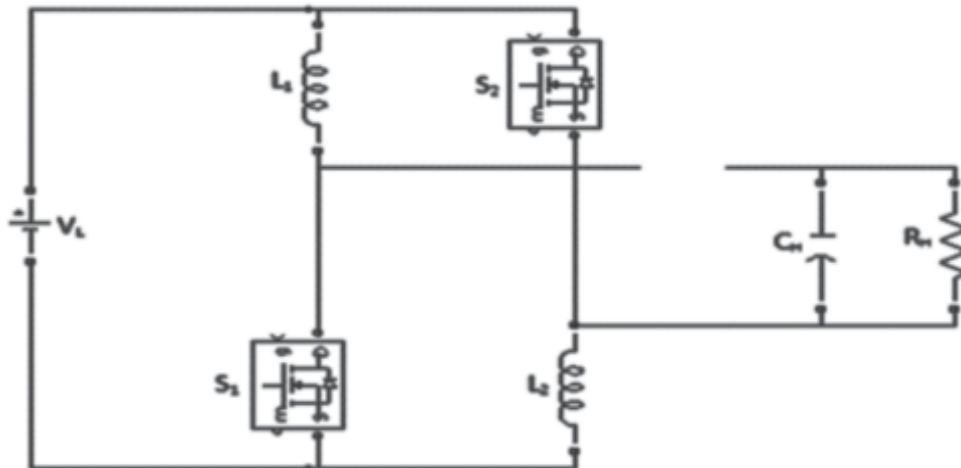


Fig. 3(b). Proposed Converter in Mode 2

The voltage side V_L and the coupled inductor are in series and their energies are transferred to capacitor C_H and to the load. Thus the voltage and current at this mode are given as follows

$$i_{L_1} = i_{L_2} \tag{7}$$

$$v_{L_1} + v_{L_2} = V_L - V_H \tag{8}$$

Substituting (3) and (4) into (8), yielding

$$\frac{di_{L_1}(t)}{dt} = \frac{di_{L_2}(t)}{dt} = \frac{V_L - V_H}{2(1+k)L}, t_1 \leq t \leq t_2 \tag{9}$$

By using the state space averaging method, the following equation is derived from (6) and (9)

$$\frac{DV_L}{(1+k)L} + \frac{(1-D)(V_L - V_H)}{2(1+k)L} = 0 \tag{10}$$

Thus the voltage gain during the step up mode is given as

$$G_{CCM(\text{step-up})} = \frac{V_H}{V_L} = \frac{1+D}{1-D} \tag{11}$$

3. SIMULATION RESULTS

The circuit diagram for boost mode is shown in Fig.4(a). The power output is measured by multiplying the output voltage and the output current. Load voltage and load current are measured using voltage and current measurement blocks respectively. The following are the assumptions made in simulation studies.

1. Internal resistance of the source is neglected.
2. Resistance of the coupled inductor is neglected.
3. ESR of the capacitor is neglected.

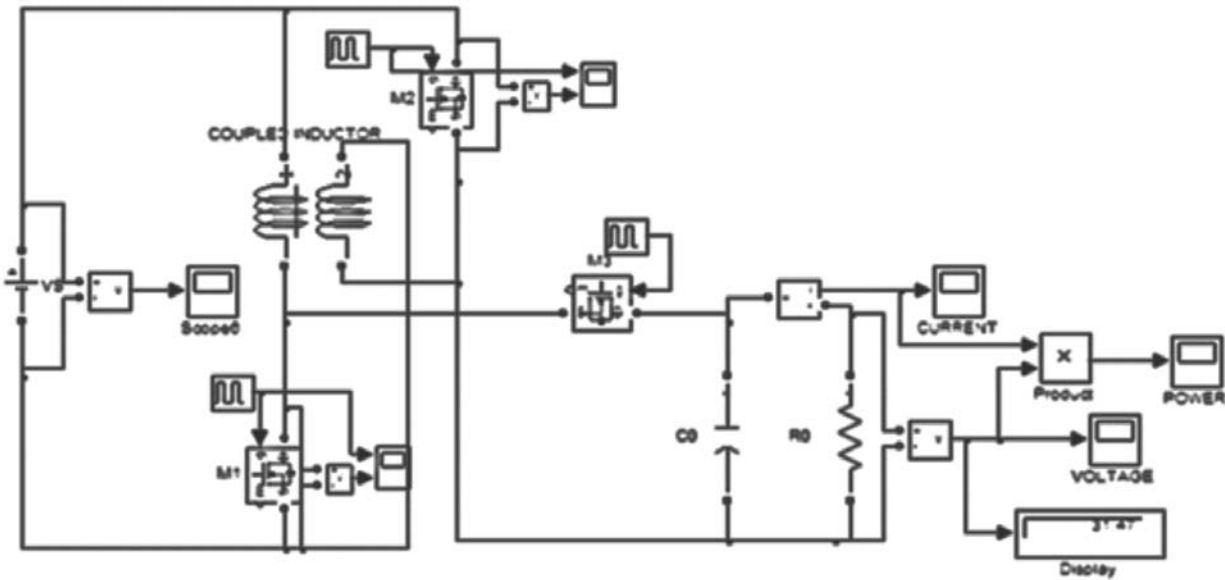


Fig. 4(a). Circuit Diagram for Boost Mode with C-Filter.

The input DC voltage is shown in Fig.4(b). The switching voltage and the voltage across the MOSFET are shown in Fig.4(c). The voltage source across the MOSFET is a compliment of the driving voltage.

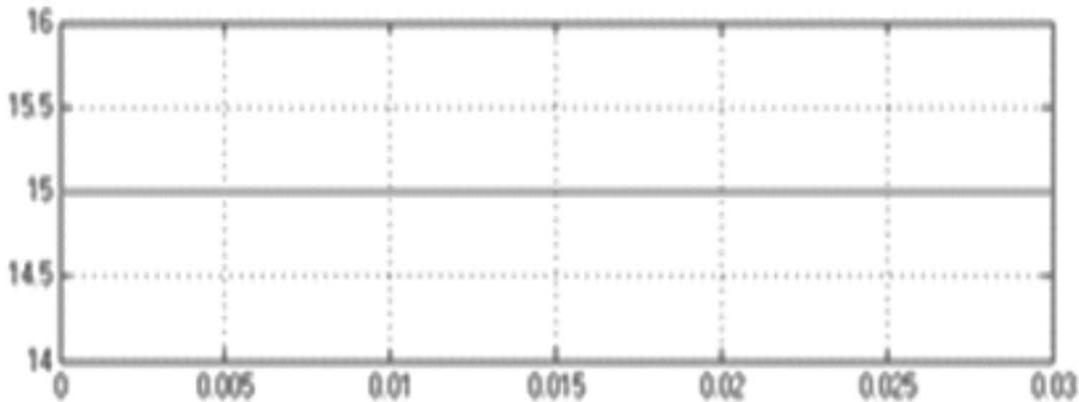


Fig. 4(b). Input Voltage

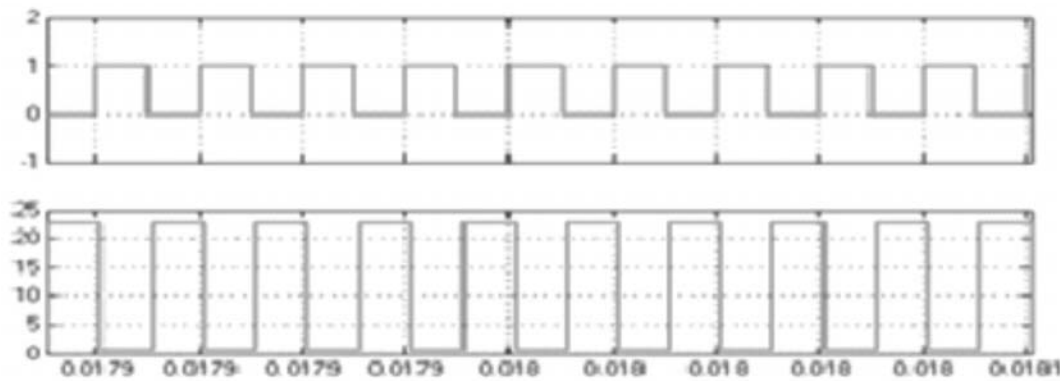


Fig. 4(c). Switching Pulse for M_1 & Voltage across the Switch V_{DS}

Switching Pulse and output voltage for M_2 are shown in Fig.4(d). The output current and output voltage are shown in Fig. 4(e) and Fig. 4(f) respectively. The output current is 2.8A and the output voltage is 30V. The output power is shown in Fig.4(g) and its value is 85 watts.

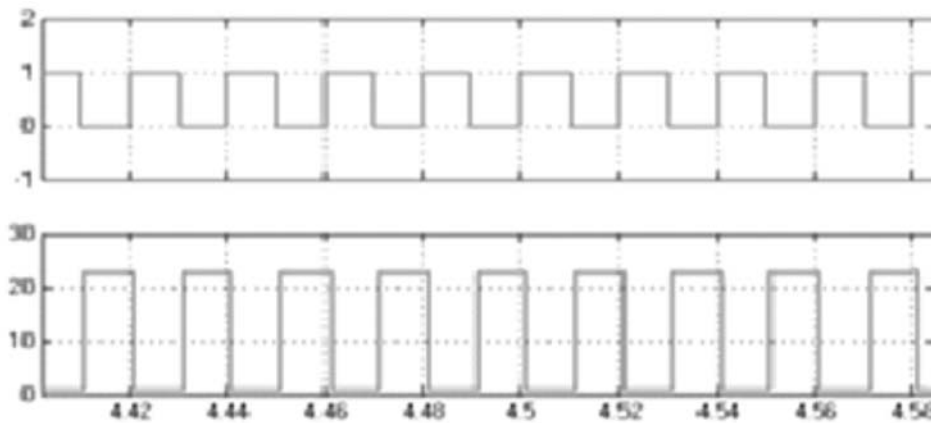


Fig. 4(d). Switching Pulse for M_2 & V_{DS}

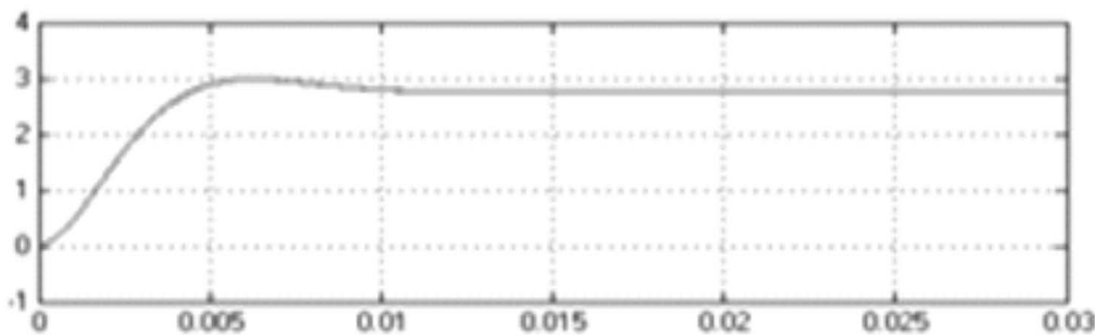


Fig. 4(e). Output Current

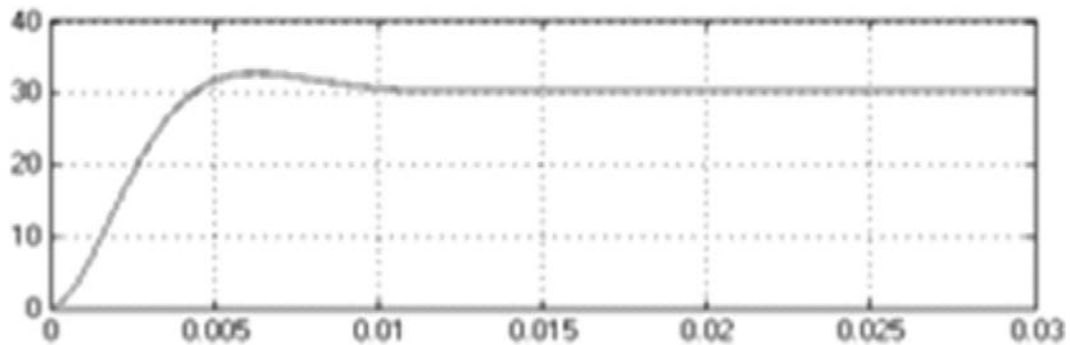


Fig. 4(f). Output Voltage

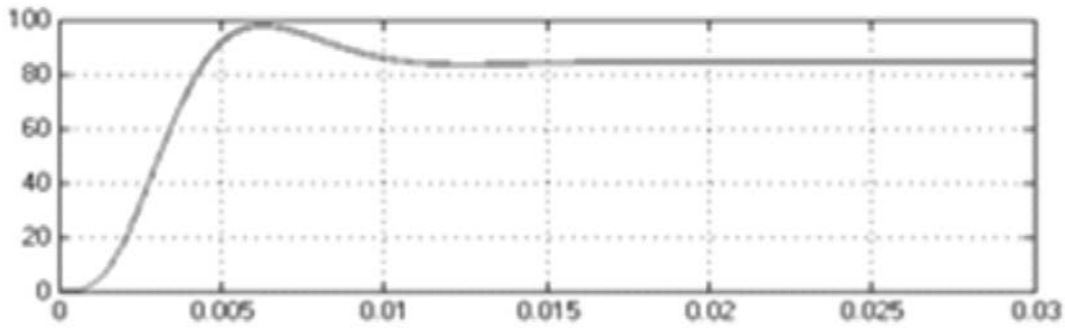


Fig. 4(g). Output Power

3.1. Open loop system

The open loop system for the boost mode using Pi-filter with a step change in input is shown in Fig.5(a). The step change in input voltage is shown in Fig.5(b). At $t = 0.5$ secs, the input voltage increases from 15V to 20V. The increase in output current, output power and output voltage are shown in Figs. 5(c), 5(d) and 5(e) respectively.

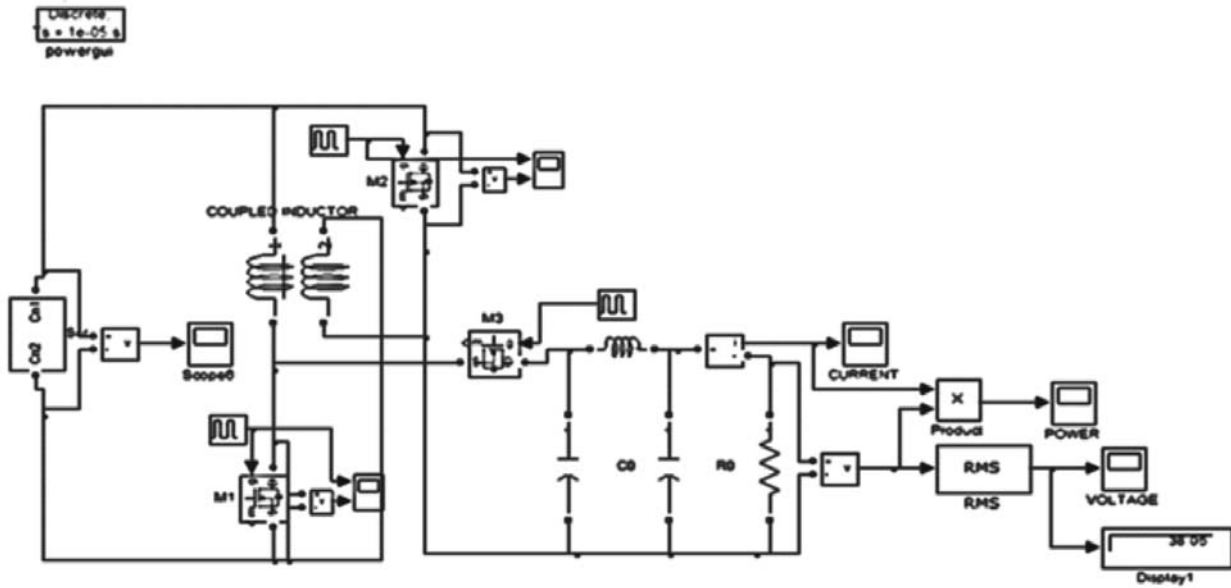


Fig. 5(a). Open loop system

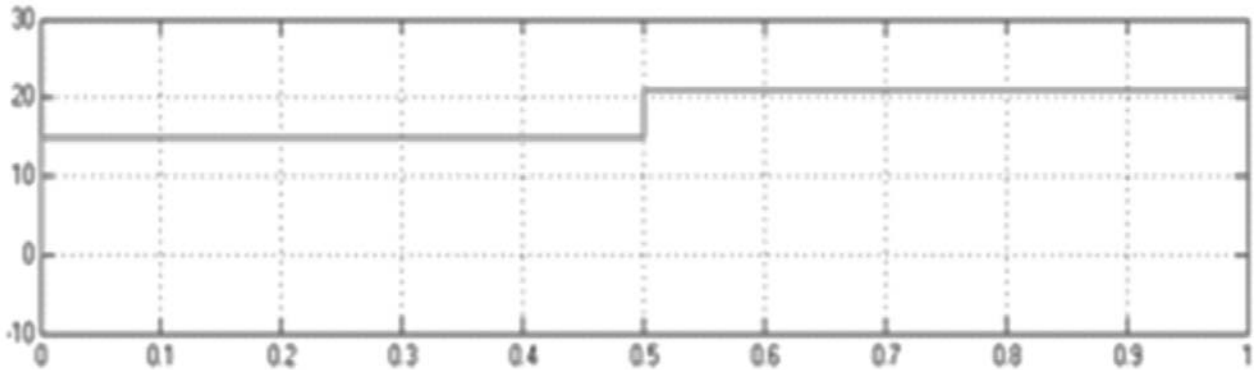


Fig. 5(b). Input Voltage

When the input voltage changes by 7V, then the output voltage changes by 10V. The steady state error is 10V. The output power increases from 85w to 185w due to increase in the input voltage. The output current increases from 3.2A to 4.8A.

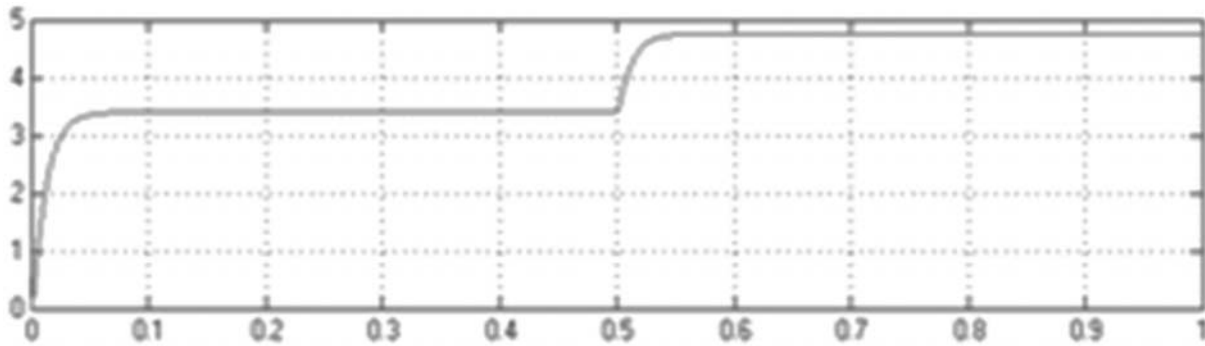


Fig. 5(c). Output Current

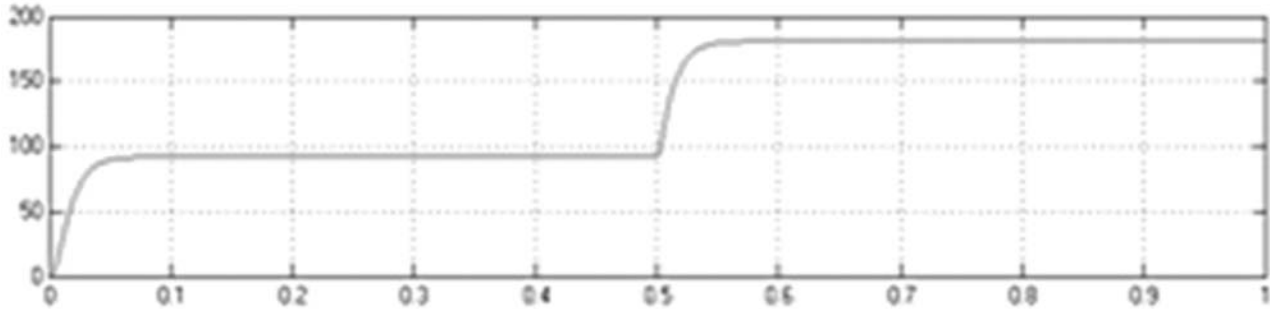


Fig. 5(d). Output Power

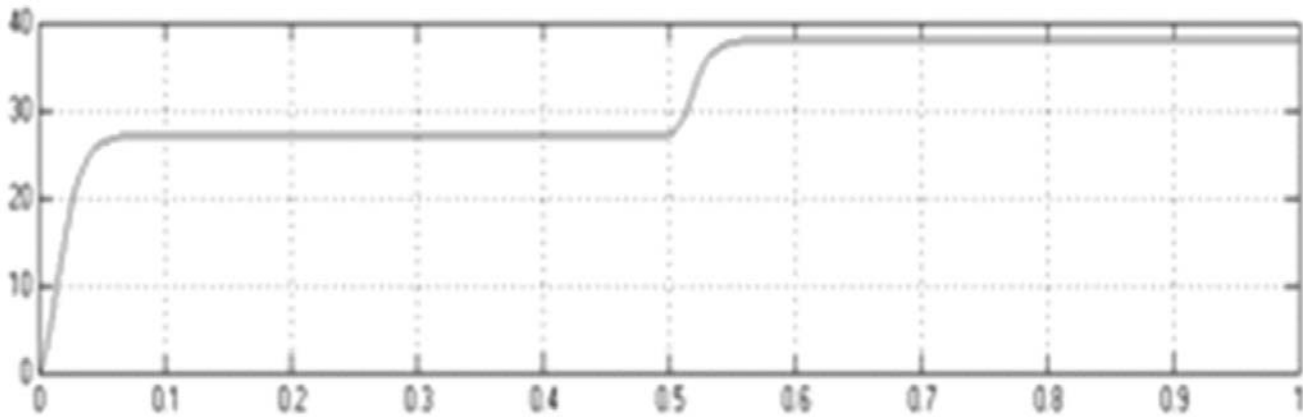


Fig. 5(e). Output Voltage

3.2. Closed loop system

The simulink diagram of closed loop system is shown in Fig. 6(a). The output voltage is sensed and it is compared with a reference voltage of 30V. The error is processed using a PI Controller. The output of PI is compared with a saw tooth waveform to generate proper pulses for M_3 . The parameters K_p and K_i are obtained using Zigler and Nicols method.

$$K_p = \frac{T}{L} = 1.5$$

and

$$K_i = 1.6L = 0.3.$$

These values are used for the simulation study.

$$V_0 = K_{pe} + K_i \int edt$$

$$V_{0(s)} = K_e E(s) + \left(\frac{K_i}{S} \right) E(s)$$

Step change in input is shown in Fig.6(b).

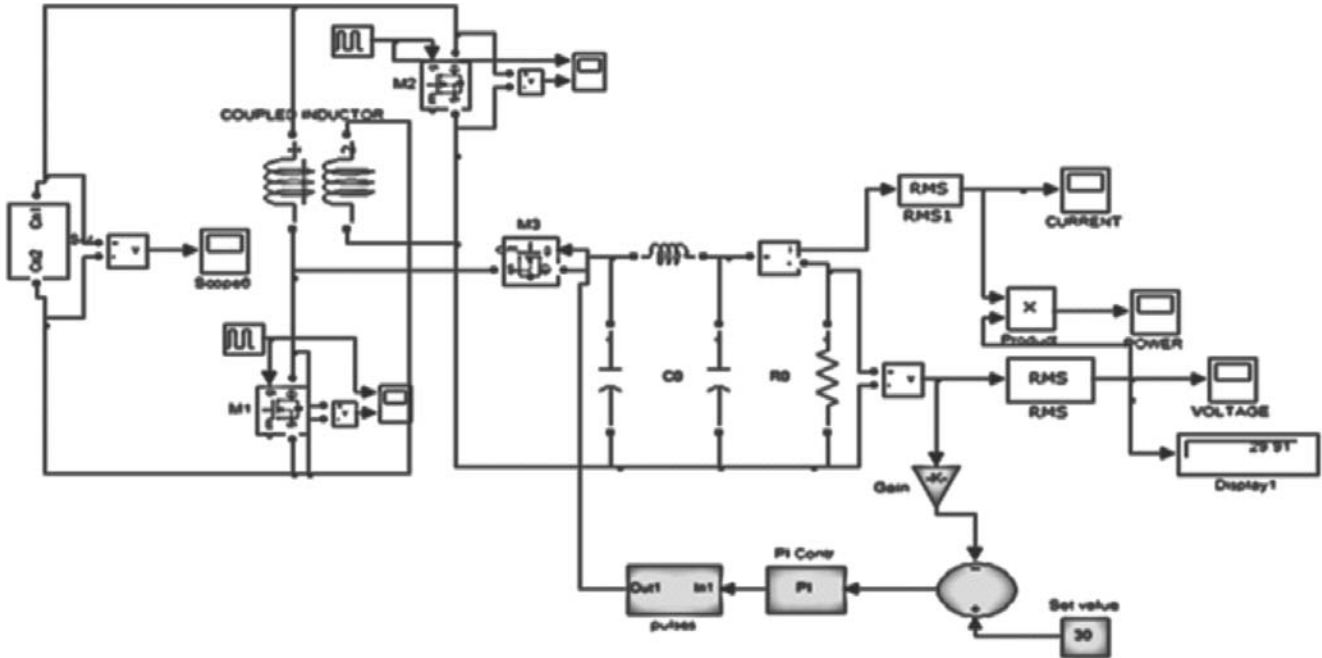


Fig. 6(a). Closed loop system

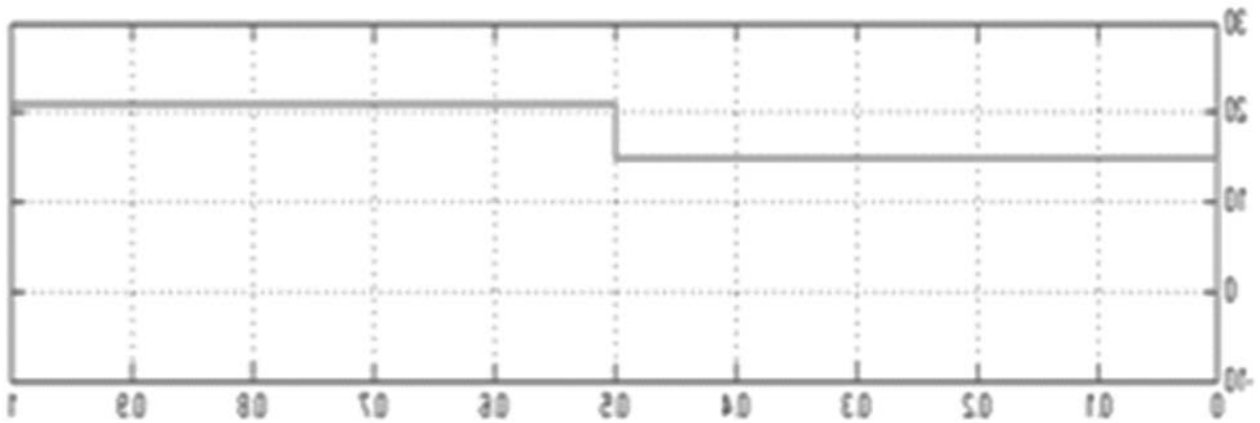


Fig. 6(b). Input Voltage

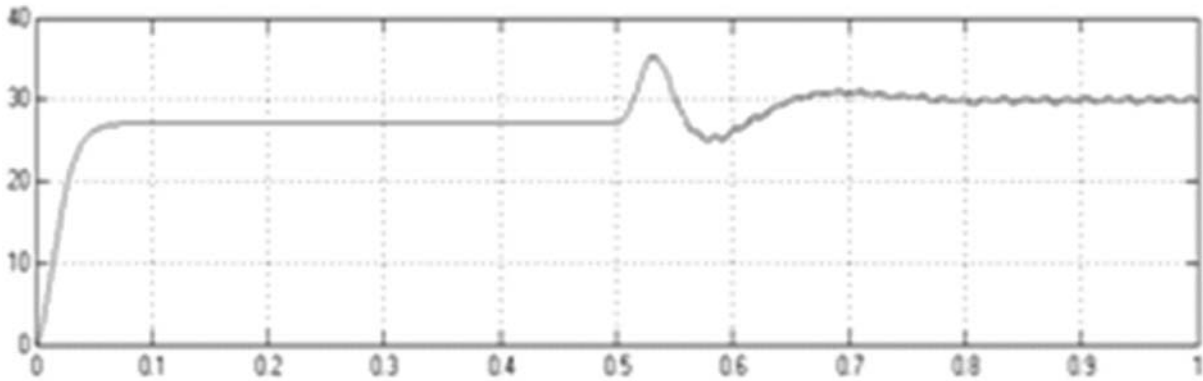


Fig. 6(c). Output Voltage

The output voltage of closed loop system is shown in Fig.6(c).The output voltage increases and then reduces to the required value. The steady state error in output voltage is 1V.This is much less than that of the open loop system. This can be further reduced by changing the amplitude and frequency of the saw tooth voltage. The peak overshoot in the output is 7V.

4. CONCLUSION

Bidirectional DC-DC converter operating in open loop and closed loop was simulated successfully with R-load. The steady state error was reduced considerably by using a closed loop system. The results obtained from the simulation suggest that the proposed bidirectional DC-DC converter is suited for electrical vehicle applications. The advantage of the system is the ability to transfer power in both the directions and reduced hardware. The disadvantage of this system is the requirement of a coupled inductor. In the present work, the closed loop system is controlled by using PI controller. The closed loop system may be controlled using Fuzzy or ANN Controller to improve the dynamic response.

5. REFERENCES

1. F. Z. Peng, H. Li, G.-J. Su, and J. S. Lawler, "A new ZVS bidirectional DC-DC converter for fuel cell and battery application," *IEEE Trans Power Electron.*, vol. 19, no. 1, pp. 54–65, Jan. 2004.
2. M. D. Jain and P. Jain, "A bidirectional DC-DC converter topology for low power application," *IEEE Trans. Power Electron.*, vol. 15, no. 4, pp. 595–606, Jul. 2000.
3. K. Ma and Y. Lee, "An integrated flyback converter for DC uninterruptible power supplies," *IEEE Trans. Power Electron.*, vol. 11, no. 2, pp. 318–327, Mar. 1996.
4. M. Jain, M. Daniele, and P. K. Jain, "A bidirectional DCDC converter topology for low power application", *IEEE Trans. Power Electron.*, vol. 15, no. 4, pp. 595-606, Jul. 2000.
5. H. Li, F.-Z. Peng, and J. S. Lawler, "A natural ZVS medium-power bidirectional DC-DC converter with minimum number of devices," *IEEE Trans. Ind. Appl.*, vol. 39, no. 2, pp. 525–535, Mar. 2003.
6. S. Inoue and H. Akagi, "A bidirectional isolated DC-DC converter as a core circuit of the next-generation medium voltage power conversion system," *IEEE Trans. Power Electron.*, vol. 22, no. 2, pp. 535–542, Mar. 2007.
7. L. Schuch, C. Rech, H. L. Hey, H. A. Grundling, H. Pinheiro, and J. R. Pinheiro, "Analysis and design of a new high-efficiency bidirectional integrated ZVT PWM converter for DC-bus and battery-bank interface," *IEEE Trans. Ind. Appl.*, vol. 42, no. 5, pp. 1321–1332, Sep. 2006.
8. P. Das, B. Laan, S. A. Mousavi, G. Moschopoulos, "A nonisolated bidirectional ZVS-PWM active clamped DCDC converter", *IEEE Trans. Ind. Appl.*, vol. 24, no. 2, pp. 553-558, Feb. 2009.
9. S. Y. Lee, G. Pfaelzer, and J. D. Wyk, "Comparison of different designs of a 42-V/14-V dc/dc converter regarding losses and thermal aspects," *IEEE Trans. Ind. Appl.*, vol. 43, no. 2, pp. 520–530, Mar./Apr. 2007.
10. K. Venkatesan, "Current mode controlled bidirectional flyback converter," in *Proc. IEEE Power Electron. Spec. Conf.*, 1989, pp. 835–842.
11. T. Qian and B. Lehman, "Coupled input-series and output-parallel dual interleaved flyback converter for high input voltage application," *IEEE Trans. Power Electron.*, vol. 23, no. 1, pp. 88–95, Jan. 2008.
12. G. Chen, Y. S. Lee, S. Y. R. Hui, D. Xu, and Y. Wang, "Actively clamped bidirectional flyback converter," *IEEE Trans. Ind. Electron.*, vol. 47, no. 4, pp. 770–779, Aug. 2000.
13. Nasiri, Z. Nie, S. B. Bekiarov, and A. Emadi, "An on-line UPS system with power factor correction and electric isolation using BIFRED converter," *IEEE Trans. Ind. Electron.*, vol. 55, no. 2, pp. 722–730, Feb. 2008.
14. M. B. Camara, H. Gualous, F. Gustin, A. Berthon, and B. Dakyo, "DC/DC converter design for supercapacitor and battery power management in hybrid vehicle applications—Polynomial control strategy," *IEEE Trans. Ind. Electron.*, vol. 57, no. 2, pp. 587–597, Feb. 2010.
15. T. Bhattacharya, V. S. Giri, K. Mathew, and L. Umanand, "Multiphase bidirectional flyback converter topology for hybrid electric vehicles," *IEEE Trans. Ind. Electron.*, vol. 56, no. 1, pp. 78–84, Jan. 2009.
16. F. Zhang and Y. Yan, "Novel forward-flyback hybrid bidirectional dc-dc converter," *IEEE Trans. Ind. Electron.*, vol. 56, no. 5, pp. 1578–1584, May 2009.
17. Jain and R. Ayyanar, "PWM control of dual active bridge: Comprehensive analysis and experimental verification," *IEEE Trans. Power Electron.*, vol. 26, no. 4, pp. 1215–1227, Apr. 2011.
18. A. Hasanzadeh, O. Onar, H. Mokhtari, and A. Khaligh, "A proportional resonant controller-based wireless control strategy with a reduced number of sensors for parallel-operated UPSs," *IEEE Trans. Power Del.*, vol. 25, no. 1, pp. 468–478, Jan. 2010.

19. Zhao, S. D. Round, and J. W. Kolar, "Full-order averaging modeling of zero-voltage-switching phase-shift bidirectional DC-DC converters," *IET Power Electron.*, vol. 3, no. 3, pp. 400-410, Mar. 2010.
20. H. Qin and J. W. Kimball, "Generalized average modeling of dual active bridge DC-DC converter," *IEEE Trans. Power Electron.*, vol. 27, no. 4, pp. 2078-2084, Apr. 2011.
21. Y. Xie, J. Sun, and J. S. Freudenberg, "Power flow characterization of a bidirectional galvanically isolated high-power dc/dc converter over a wide operating range," *IEEE Trans. Power Electron.*, vol. 25, no. 1, pp. 54-66, Jan. 2010.
22. D. Kim, S. H. Paeng, J. W. Ahn, E. C. Nho, and J. S. Ko, "New bidirectional ZVS PWM sepic/zeta dc-dc converter," in *Proc. IEEE ISIE*, 2007, pp. 555-560.
23. R. J. Wai and R. Y. Duan, "High-efficiency bidirectional converter for power sources with great voltage diversity," *IEEE Trans. Power Electron.*, vol. 22, no. 5, pp. 1986-1996, Sep. 2007.
24. L. S. Yang, T. J. Liang, and J. F. Chen, "Transformerless dc-dc converters with high step-up voltage gain," *IEEE Trans. Ind. Electron.*, vol. 56, no. 8, pp. 3144-3152, Aug. 2009.
25. D. Costinett, D. Maksimovic, and R. Zane, "Design and control for high efficiency in high step-down dual active bridge converters operating at high switching frequency," *IEEE Trans. Power Electron.*, vol. 28, no. 8, pp. 3931-3940, Aug. 2013.
26. K.C.Ramya and V.Jegathesan, "Reduction of Ripple in the Bidirectional DC-DC Converter with the Coupled Inductor," *International Journal of Innovative Research in Science, Engineering and Technology* Vol. 4, Issue 2, pp 434-441., February 2015.
27. Lung-Sheng Yang and Tsorng-Juu Liang, "Analysis and Implementation of novel bidirectional dc-dc converter," *IEEE Trans. Ind. Electron.*, vol. 59, no. 1, Jan. 2012.